High-Efficient Rectifier With Extended Input Power Range Based on Self-Tuning Impedance Matching

Pengde Wu, Shao Ying Huang, *Member, IEEE*, Wenshen Zhou, Zhi Hua Ren, Zhenlong Liu, Kama Huang, and Changjun Liu, *Senior Member, IEEE*

***Abstract*— In this letter, a microwave rectifier with a wide input power range is presented by proposing a self-tuning impedance matching (STIM). The STIM consists of a varactor reversely biased by the output voltage of the rectifier to compensate the variation of the input impedance caused by the input power, so that impedance matching is obtained over a wider input power range. For validation, the proposed rectifier at 2.4 GHz was designed and implemented. The experimental results show that the RF-dc power conversion efficiency maintains over 50% and 70% within the input power ranges of 2.5–25.5 dBm and 11–24.5 dBm, respectively. Compared with the counterpart without the STIM, an improvement of 7.2 dB in terms of the input power range when the reflection coefficient is less than −10 dB was successfully demonstrated.**

***Index Terms*— High efficiency, RF rectifier, self-tuning impedance matching (STIM), wide input power range, wireless power transfer (WPT).**

I. Introduction

THE wireless power transfer (WPT) and energy harvesting are promising microwave/RF technologies that are able to extend the battery life of a device and allow applications where wired power is hard to access or unavailable. A rectenna is one of the key components in WPT/energy harvesting, which is a combination of a rectifier and an antenna. However, due to the working environment, the input microwave power of a rectenna generally fluctuates, e.g., a rectenna attached to an aircraft [1]. Consequently, the input impedance of the nonlinear rectifying diodes in a rectifier varies with the input power, resulting in an impedance mismatch and a severe drop of RF-dc power conversion efficiency (PCE).

Recently, mainly three approaches have been proposed to reduce the sensitivity of the rectifying efficiency to input power variation. They are through increasing the breakdown voltage of a rectifying diode [2], [3], introducing power recycling [4], [5], and reducing the variation of input impedance caused by the input power [6]. In [2] and [3], a GaAs pHENT and a MOSEFT are adopted to extend the breakdown voltage of the rectifying diode, respectively. For this approach, it is noted that the working frequency range of the rectifier is limited by the circuit components introduced. For adding a power recycling network, in [4], a balance configuration of rectifier was proposed and a high-efficiency power recycler was presented. In [5], a subrectifier dealing with lower power level is connected to the isolation port of a branch-line coupler to extend the input power range. For the approach of introducing a power recycling network, additional circuit area is needed. Moreover, the circuit complexity increases and additional insertion loss is introduced. In terms of reducing the variation of input impedance, in [6], a resistance compression network (RCN) was introduced and a wide input power ranger was obtained. Although the introduction of the RCN lowers the sensitivity of the rectifier to the input power or to the load, RCN does not compensate the change in the input impedance based on the change of the input power. Moreover, it is a resistive network that introduces additional insertion loss.

In this letter, a self-tuning impedance matching (STIM) circuit is proposed to design a rectifier with a high immunity to the input power fluctuation. It leads to a rectifier with a significant increase in the input power range. In the STIM, a nonresistive varactor is adaptively controlled by the input power of the rectifier to compensate the change of the input impedance caused by the fluctuation of the input power.

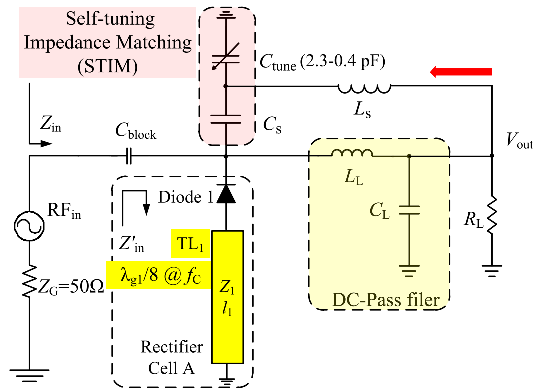

Fig. 1. Schematic of the proposed rectifier with an STIM.

II. Design and Simulation

Fig. 1 shows the block diagram of the proposed rectifier with an STIM. It consists of a dc block capacitor (C_{block}), the STIM, a rectifier Cell A, a dc-Pass filter, and a dc load R_L, from left to right. The output dc voltage is proportional to the input power. It is fed back to the STIM to control the varactor, C_{tune}. Next, the variation of the input impedance with the input power of a shunt diode rectifier will be discussed, and the design and function of the proposed STIM will be presented.

Manuscript received May 28, 2018; accepted October 10, 2018. Date of publication November 6, 2018; date of current version December 4, 2018. This work was supported by NFSC under Grant 61271074. *(Corresponding authors: Shao Ying Huang; Changjun Liu.)*

P. Wu, Z. Liu, K. Huang, and C. Liu are with the School of Electronics and Information Engineering, Sichuan University, Chengdu 610064, China (e-mail: cjliu@ieee.org).

S. Y. Huang, W. Zhou, and Z. H. Ren are with the Pillar of Engineering Product Development, Singapore University of Technology and Design, Singapore 487372 (e-mail: huangshaoying@sutd.edu.sg).

Color versions of one or more of the figures in this paper are available online at http://ieeexplore.ieee.org.

Digital Object Identifier 10.1109/LMWC.2018.2876773

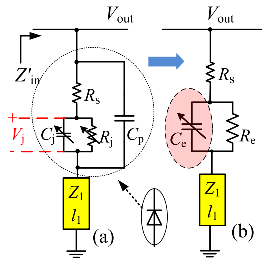

Fig. 2. (a) Detailed and (b) simplified circuit of Cell A.

A. Input Impedance Variation of the Rectifier Cell A

In Fig. 1, the input impedance of rectifier Cell A varies with the input power. As shown in Fig. 1, it consists of a Schottky diode (HSMS-282B, denoted as Diode 1) and a short-circuited microstrip line stub (TL_1) for impedance matching. TL_1 has a characteristic impedance of Z_1 and an electric length of $\lambda_{g1}/8$ at the working frequency, f_{1c}. With a length of $\lambda_{g1}/8$, at f_{1c}, the input impedance of TL_1 equals Z_1 [7]. The frequency f_{1c} is set to be 2.4 GHz. The input impedance of the rectifier (Cell A) is denoted as Z'_{in}. At an input power of 20 dBm, the rectifier is matched ($\text{Im}(Z'_{\text{in}}) = 0$) at f_{1c} by tuning Z_1 to change the input impedance of TL_1 so as to compensate the capacitance of Diode 1. However, Z'_{in} varies with the input power. Following is an analysis using both numerical calculation based on a linear circuit model and the harmonic balance simulation in Advanced Designed System (ADS, Keysight) based on a nonlinear SPICE model.

Fig. 2(a) and (b) shows a detailed linear circuit model of Cell A and its simplified version, respectively. In Fig. 2(a), R_s denotes the series resistance, R_j is the junction resistance, and C_p is the package capacitance. The junction capacitance C_j is proportional to $1/\sqrt{(V_j + V_D)}$, where V_j is the junction voltage and V_D is the built-in voltage of Diode 1. In other words, the impedance of the diode varies with the reversed biased dc voltage, the dc output V_{out}. Therefore, the input impedance of Cell A, Z'_{in}, varies with the input power based on the fact that V_{out} varies with the input power.

In Fig. 2(b), for a numerical analysis, the equivalent circuit for a packed Schottky diode is simplified as a resistor R_e in parallel with a capacitor C_e that increases with a decrease in V_{out} and a low input power. R_e is assumed to be a constant 400 Ω to simplify the calculation, and C_p is relatively small and is equivalent as open circuit. With the simplified equivalent circuit, the input impedance Z'_{in} can be described by (1)

$$Z'_{\text{in}} = Z_S + jZ_1 \tag{1}$$

where Z_S is the total impedance of the Schottky diode. As the Schottky diode is modeled as C_e and R_e in parallel, Z_S is expressed as

$$Z_S = \frac{R_e}{1 + (R_e C_e \omega)^2} - j\frac{R_e^2 C_e \omega}{1 + (R_e C_e \omega)^2} \tag{2}$$

where ω is the angular frequency. Substituting (2) to (1), the imaginary part of Z'_{in} is expressed as follows:

$$\text{Im}(Z'_{\text{in}}) = -\frac{R_e^2 \omega}{1/C_e + C_e(R_e\omega)^2} + Z_1. \tag{3}$$

As can be seen in (3), for a given C_e and R_e, $\text{Im}(Z'_{\text{in}})$ can be zeroed by tuning Z_1. When the input power decreases, V_{out} decreases and C_e increases. The value of $(1/C_e + C_e(R_e\omega)^2)$ increases with C_e ($C_e > 1/(R_e\omega)$), which leads to a decrease in the first term in (3) and Z'_{in} becomes inductive.

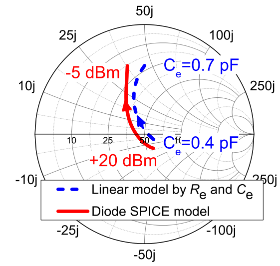

Fig. 3. Z'_{in} versus the input power.

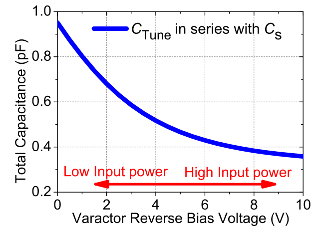

Fig. 4. Total capacitance of STIM versus the reverse bias voltage.

At 2.4 GHz, the calculated Z'_{in} varies from $(58.6 - j5)\ \Omega$ to $(16.5 + j56)\ \Omega$ when C_e changes from 0.4 to 0.7 pF (the input power decreases) and R_e is a constant. Fig. 3 plots Z'_{in} over the variation of C_e.

The harmonic balance simulations in ADS based on the nonlinear SPICE model was performed. Z'_{in} varies from $(56.6 - j15)\ \Omega$ to $(17.6 + j36)\ \Omega$ for an input power from 20 to -5 dBm at 2.4 GHz. It is also plotted in Fig. 3. As shown in Fig. 3, the harmonic balance simulation results agree with the numerical calculation based on the linear equivalent circuit. Both results indicate that Z'_{in} is more inductive at low power. Therefore, to compensate this change, higher capacitance is needed at a low input power.

B. Self-Tuning Input Impedance Matching

As analyzed, the input impedance of a rectifier varies with its input power. Here, an adaptive STIM circuit is proposed in parallel with the rectifier and controlled by the output voltage. It is designed so that when the rectifier has a low input power, the STIM has an increased capacitance adaptively to compensate an increase in the inductance of the rectifier (Cell A) for matching. The adaptive tuning of capacitance in the STIM is implemented by a varactor C_{tune} controlled through the rectifier output V_{out}, as shown in Fig. 1.

Fig. 4 shows the total capacitance of the STIM versus the reverse bias voltage of the varactor where a low input power corresponds to a low reverse bias voltage. As shown, when the input power is low, the total capacitance of the STIM goes high, which is used to compensate an increase in the inductance of the rectifier as shown in Fig. 3.

Fig. 5 shows the simulated $|S_{11}|$ versus the input power. It can be observed that the lower bound of the input power range for $|S_{11}| < -10$ dB is enhanced from 4 to -4 dBm by the proposed STIM (an improvement of 8 dBm). Moreover, it is noted that $|S_{11}|$ slightly increases when the input power goes beyond 10 dBm.

III. Implementation and Measurements

The proposed rectifier was fabricated and tested. The layout and a photograph of the fabricated rectifier are shown in Fig. 6. Rogers 4350B ($\epsilon_r = 3.66$ and $\tan\delta = 0.002$) was used as the substrate. As can be seen, the Schottky diode with a short circuit stub (TL_1) is connected to the STIM directly.

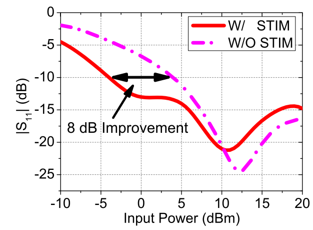

Fig. 5. Simulated return loss with and without the STIM.

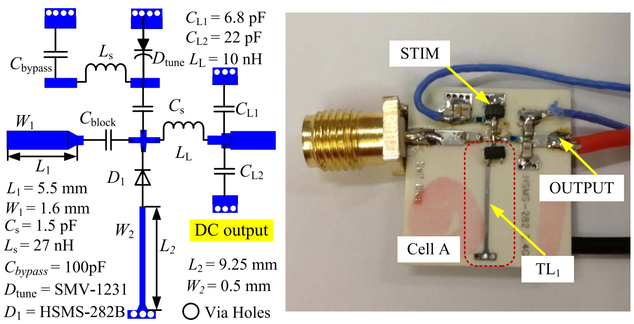

Fig. 6. The layout and a photograph of the proposed diode array.

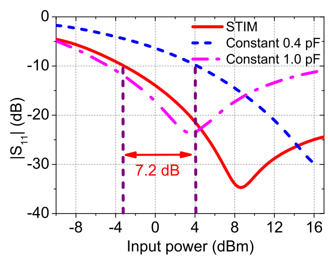

Fig. 7. Measured $|S_{11}|$ of the rectifiers with and without STIM.

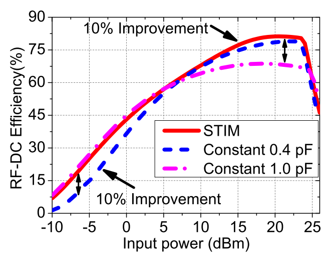

Fig. 8. Measured PCE of the rectifiers with and without STIM.

TABLE I

COMPARISON WITH THE PRIOR RECTIFIERS

Reference		[8]	[9]	[10]	This work
Power range for efficiency over 70%		8.4 dB	3 dB	8.6 dB	13.5 dB
Power range for efficiency over 50%		21.3 dB	12 dB	17.3 dB	23 dB
Peak Eff.	Eff.	80%	73.5%	80.8%	81.2%
	Power	28.5 dBm	23 dBm	17.2 dBm	20.5 dBm
	Fre.	2.45 GHz	2.3 GHz	2.45 GHz	2.4 GHz
Rectifier Element		HSMS282	HSMS282	HSMS286	HSMS282
Number of diode		4	1	4	1
Dimension (mm×mm)		82×66	65×26	N.A.	30×19

In addition, a capacitor C_{block} (22 pF) was used for dc block, and the load R_L is 400 Ω.

Fig. 7 shows the measured $|S_{11}|$ from −10 to 17 dBm using a vector network analyzer (VNA, Keysight N5249B). The upper limit of the input power is imposed by the VNA. For the rectifier with the STIM, $|S_{11}|$ is well below −10 dB for input powers from 3.1 to 17 dBm at 2.4 GHz. The input power range is 7.2 dB wider than the reciter without the STIM where a capacitor of 0.4 and 1.0 pF was used to replace the STIM. Significant improvements can be observed, especially when the input power is low (−10–0 dBm).

Fig. 8 depicts the measured PCE versus input power at 2.4 GHz. Compared to the case with 0.4 pF, the STIM leads to a 10% improvement of PCE at a low input power (−10–0 dBm). As observed, the measured PCE of the proposed rectifier with the STIM is more than 50% within the input power range from 2.5 to 25.5 dBm. An efficiency of over 70% is also obtained in the input power range of 11 to 24.5 dBm for the proposed rectifier. The maximum measured PCE of the proposed rectifier is 81.2% at 20.5 dBm.

Table I shows a comparison of the performances between the proposed rectifier and those reported in the literature working at 2.4 GHz. As shown, the proposed topology shows the widest input power range for the efficiency of higher than 50% in caparison with others. Meanwhile, only one diode is used and the physical size is 30 mm × 19 mm, which is the smallest among the four structures.

IV. CONCLUSION

A high-efficiency microwave rectifier with an extended input power range is presented. STIM is proposed. By using STIM, 10% improvement of PCE at a low input power can be achieved. Meanwhile, the input power range when $|S_{11}| < -10$ dB is 7.2 dB wider than the counterparts. Moreover, the proposed STIM is in parallel with the rectifier cell. Therefore, no additional insertion loss is introduced. Compared to other reported rectifiers with a wide input power range, the proposed topology has shown an increase in the operating power range.

REFERENCES

[1] M. Iwashimizu *et al.*, "Study on direction detection in a microwave power transmission system for a Mars observation airplane," in *Proc. IEEE Wireless Power Transf. Conf.*, May 2014, pp. 146–149.

[2] Z. Liu, Z. Zhong, and Y.-X. Guo, "Enhanced dual-band ambient RF energy harvesting with ultra-wide power range," *IEEE Microw. Wireless Compon. Lett.*, vol. 25, no. 9, pp. 630–632, Sep. 2015.

[3] H. C. Sun, Z. Zhong, and Y. X. Guo, "Design of rectifier with extended operating input power range," *Electron. Lett.*, vol. 49, no. 18, pp. 1175–1176, Aug. 2013.

[4] M.-D. Wei, Y.-T. Chang, D. Wang, C.-H. Tseng, and R. Negra, "Balanced RF rectifier for energy recovery with minimized input impedance variation," *IEEE Trans. Microw. Theory Techn.*, vol. 65, no. 5, pp. 1598–1604, May 2017.

[5] Y. Y. Xiao, Z.-X. Du, and X. Y. Zhang, "High-efficiency rectifier with wide input power range based on power recycling," *IEEE Trans. Circuits Syst. II, Exp. Briefs*, vol. 65, no. 6, pp. 744–748, Jun. 2018.

[6] C. Song, Y. Huang, J. Zhou, and P. Carter, "Improved ultrawideband rectennas using hybrid resistance compression technique," *IEEE Trans. Antennas Propag.*, vol. 65, no. 4, pp. 2057–2062, Apr. 2017.

[7] C. Liu, F. Tan, H. Zhang, and Q. He, "A novel single-diode microwave rectifier with a series band-stop structure," *IEEE Trans. Microw. Theory Techn.*, vol. 65, no. 2, pp. 600–606, Feb. 2017.

[8] Z.-X. Du and X. Y. Zhang, "High-efficiency microwave rectifier with less sensitivity to input power variation," *IEEE Microw. Wireless Compon. Lett.*, vol. 27, no. 11, pp. 1001–1003, Nov. 2017.

[9] D. Wang and R. Negra, "A 2.3 GHz single-ended energy recovery rectifier with stepped-impedance resonator for improved efficiency of outphasing amplifier," in *Proc. Eur. Microw. Conf.*, Oct. 2013, pp. 920–923.

[10] X. Y. Zhang, Z.-X. Du, and Q. Xue, "High-efficiency broadband rectifier with wide ranges of input power and output load based on branch-line coupler," *IEEE Trans. Circuits Syst. I, Reg. Papers*, vol. 64, no. 3, pp. 731–739, Mar. 2017.